Chapter 5

The BTeV Detector

R. Kutschke, for the BTeV Collaboration [1]

5.1 Introduction

On May 15, 2000 the BTeV Collaboration submitted their proposal [2] to the Fermilab management and on June 27, 2000 the Fermilab director announced that BTeV experiment had been given Stage I approval. The information given in this chapter is abstracted from that proposal. Much additional information is available in the proposal, including the physics case for the experiment, a detailed description of the proposed detector, a description of the simulation tools used to evaluate the detector design, a summary of the physics reach, a cost estimate and extensive appendices.

This chapter will discuss the reasons for choosing a forward detector, followed by overviews of the detector, the simulation tools and the analysis software. Some illustrative results will also be included. As discussed in section 2.4 of this report, all BTeV event yields were computed under the presumption that the cross-section for $b\bar{b}$ production at the Tevatron is 100 μb. All effieciencies and background levels were computed for an average 2 interactions per beam crossing, which corresponds to a luminosity of 2×10^{32} cm^{-2}s^{-1} and an interval of 132 ns between beam crossings.

5.2 Rationale for a Forward Detector at the Tevatron

The BTeV detector is a double arm forward spectrometer which covers from 10 to 300 mrad, with respect to the colliding beam axis.[1] It resembles a pair of fixed target detectors arranged back-to-back. In Section 2.1 of the BTeV proposal [2] the reasons for this choice are explained in detail; a summary is presented here.

According to QCD calculations of b quark production, there is a strong correlation between the B momentum and pseudorapidity, η. Near η of zero, $\beta\gamma \approx 1$, while at larger values of $|\eta|$, $\beta\gamma$ can easily reach values well beyond 6. This is important because the mean decay length increases with $\beta\gamma$ and, furthermore, the momenta of the decay products are larger, suppressing multiple scattering errors. As discussed in section 2.8.1 this is most important in the trigger.

[1] BTeV refers to both the proton direction and the antiproton directions as forward.

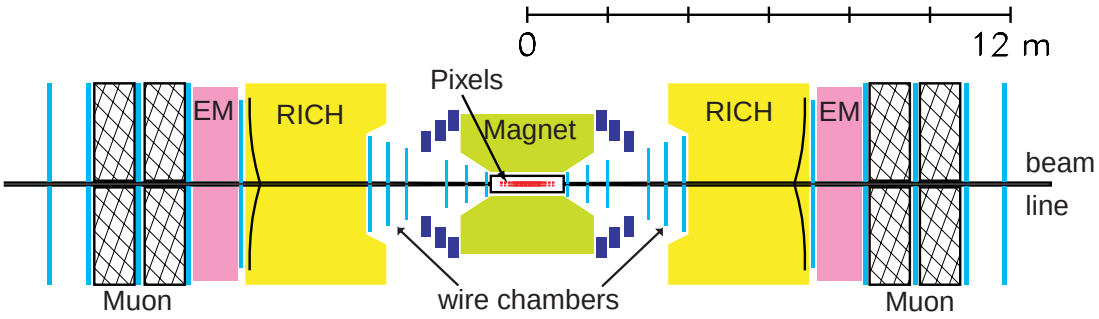

Figure 5.1: A sketch of the BTeV detector. The two arms are identical.

A crucially important attribute of $b\bar{b}$ production at hadron colliders is that the η of the b hadron and that of its companion $\bar{b}$ hadron are strongly correlated: when the decay products of a b-flavored hadron are within the acceptance of one arm of the spectrometer, the decay products of the accompanying $\bar{b}$ are usually within the acceptance of the *same* arm of the detector. This allows for reasonable levels of flavor tagging.

The long B decay length, the correlated acceptance for both b hadrons and the suppression of multiple scattering errors make the forward direction an ideal choice.

5.3 Detector Description

A sketch of the BTeV detector is shown in Fig. 5.1. The geometry is complementary to that used in current collider experiments. The detector looks similar to a fixed target experiment, but has two arms, one along the proton direction and the other along the antiproton direction.

The key design features of BTeV include:

- A dipole located on the IR, which gives BTeV an effective "two arm" acceptance;
- A precision vertex detector based on planar pixel arrays;
- A detached vertex trigger at Level 1 that makes BTeV efficient for most final states, including purely hadronic modes;
- Excellent particle identification using a Ring Imaging Cherenkov Detector (RICH);
- A high quality $PbWO_4$ electromagnetic calorimeter capable of reconstructing final states with single photons, π^o's, η's or η''s; it can also identify electrons;
- Precision downstream tracking using straw tubes and silicon microstrip detectors, which provide excellent momentum and mass resolution;
- Excellent identification of muons using a dedicated detector with the ability to supply a dimuon trigger; and

- A very high speed and high throughput data acquisition system which eliminates the need to tune the experiment to specific final states.

Each of these key elements of the detector is discussed in detail in Part II of the proposal [2] and is discussed briefly below.

5.3.1 Dipole Centered on the Interaction Region

A large dipole magnet, bending vertically and with a 1.6 T central field, is centered on the interaction region. This is the most compact way to provide momentum measurements in both arms of the spectrometer. Moreover the pixel detector is inside the magnetic field, which gives the Detached Vertex Trigger the capability of rejecting low momentum tracks. Such tracks undergo large multiple Coulomb scattering and might sometimes be misinterpreted as detached tracks.

5.3.2 The Pixel Vertex Detector

In the center of the magnet there is a silicon pixel vertex detector. This detector serves two functions: it is an integral part of the charged particle tracking system, providing accurate vertex information for the offline analysis; and it delivers very clean, precision space points to the BTeV vertex trigger.

BTeV has tested prototype pixel devices in a test beam at Fermilab. These devices consist of 50 μm $\times$ 400 μm pixel sensors bump-bonded to custom made electronics chips, developed at Fermilab. The position resolution achieved in the test beam is shown in Fig. 5.2; overlayed on that figure is resolution function used in the Monte Carlo simulation. The measured resolution is excellent and exceeds the requirement of 9 μm.

The critical quantity for a b experiment is L/σ_L, where L is the distance between the primary (interaction) vertex and the secondary (decay) vertex, and σ_L is its error. The efficacy of this geometry is illustrated by considering the distribution of the resolution on the B decay length, L, for the decay $B^o \to \pi^+\pi^-$. Fig. 5.3 shows the r.m.s. error in the decay length as a function of momentum; it also shows the momentum distribution of the B's accepted by BTeV. The following features are noteworthy:

- The B's used by BTeV peak at $p = 30$ GeV/c and average about 40 GeV/c.
- The mean decay length is equal to 450 μm $\times\, p/M_B$.
- The error on the decay length is smallest near the peak of the accepted momentum distribution. It increases at lower values of p, due to multiple scattering, and increases at larger values of p due to the smaller angles of the Lorentz-boosted decay products.

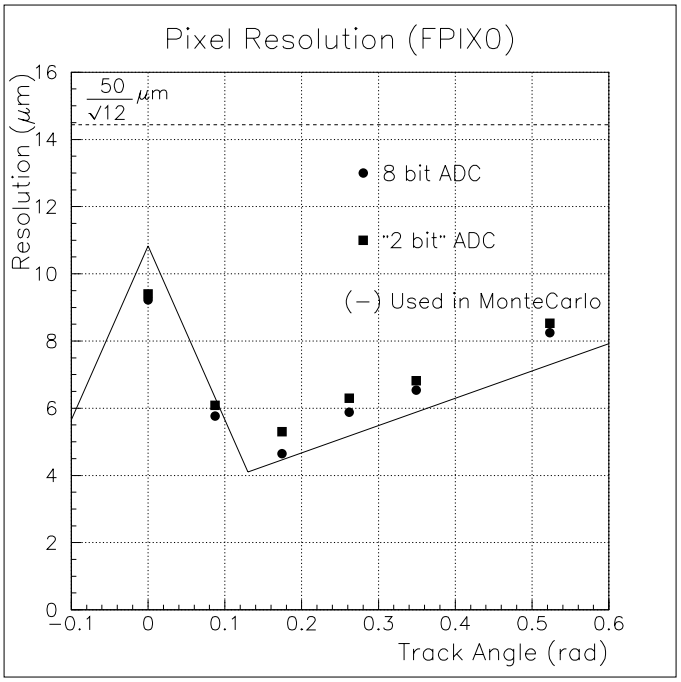

Figure 5.2: The resolution achieved in the test beam run using 50 μm wide pixels and an 8-bit ADC (circles) or a 2-bit ADC (squares), compared with the simulation (line).

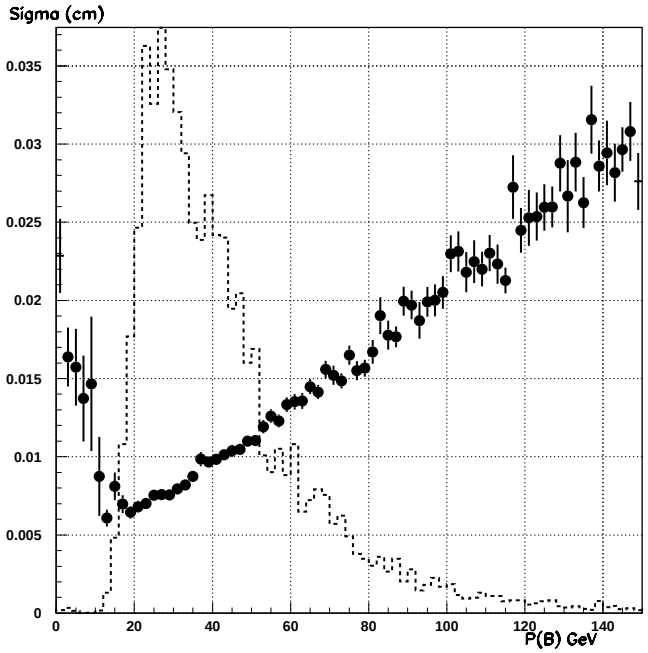

Figure 5.3: The B momentum distribution for $B^o \to \pi^+\pi^-$ events (dashed) and the error in decay length σ_L as a function of momentum.

Process	Eff. (%)
Minimum bias	1
$B_s \to D_s^+ K^-$	74
$B^0 \to D^{*+}\rho^-$	64
$B^0 \to \rho^0\pi^0$	56
$B^0 \to J/\psi K_s$	50
$B_s \to J/\psi K^{*o}$	68
$B^- \to D^0 K^-$	70
$B^- \to K_s\pi^-$	27
$B^0 \to$ 2-body modes	63
$(\pi^+\pi^-, K^+\pi^-, K^+K^-)$	

Table 5.1: Level 1 trigger efficiencies for minimum-bias events and for various processes of interest. For the minimum bias events the efficiency is quoted as a percentage of all events but for the signal channels the efficiencies are quoted as a percentage of those events which pass the offline analysis cuts. All trigger efficiencies are determined for an average of two interactions per crossing.

5.3.3 The Detached Vertex Trigger

It is impossible to record data from each of the 7.5 million beam crossings per second. A prompt decision, colloquially called a "trigger," must be made to record or discard the data from each crossing. The main BTeV trigger is provided by the silicon pixel detector. The Level 1 Vertex Trigger inspects every beam crossing and, using only data from the pixel detector, reconstructs the primary vertices and determines whether there are detached tracks which could signify a B decay. Since the b's are at high momentum, the multiple scattering of the decay products is minimized, allowing for triggering on detached heavy quark decay vertices.

With outstanding pixel resolution, it is possible to trigger efficiently at Level 1 on a variety of b decays. The trigger has been fully simulated, including the pattern recognition code. Table 5.1 summarizes the results of the trigger simulations. The trigger efficiencies are generally above 50% for the b decay states of interest and at the 1% level for minimum bias background. The efficiencies for signal channels are quoted as a percentage of events which pass the offline analysis cuts. This is an appropriate statistic because most of the b decays are not useful for doing physics: their decay products lie outside of the fiducial volume of the detector, their decay lengths are not long enough, their decay products can be ambiguously assigned to several candidate vertices and so on. Separate Monte Carlo runs were performed to measure overall event rates and bandwidth requirements and to ensure that the trigger is efficient for generic b and c decays.

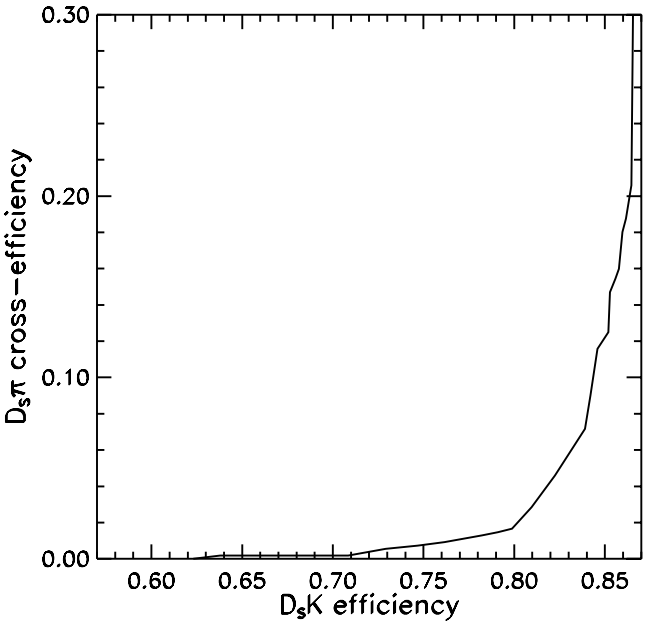

Figure 5.4: The efficiency to detect the fast K^- in the reaction $B_s \to D_s^+ K^-$ versus the rate to misidentify the π^- from $B_s \to D_s^+ \pi^-$ as a K^-.

5.3.4 Charged Particle Identification

Charged particle identification is an absolute requirement for an experiment designed to study the decays of b and c quarks. The relatively open forward geometry has sufficient space to install a Ring Imaging Cherenkov detector (RICH), which provides powerful particle ID capabilities over a broad range of momentum. The BTeV RICH detector must separate pions from kaons and protons in a momentum range from 3 to 70 GeV/c. The lower momentum limit is determined by soft kaons useful for flavor tagging, while the higher momentum limit is given by two-body B decays. Separation is accomplished using a gaseous freon radiator to generate Cherenkov light in the optical frequency range. The light is then focused by mirrors onto Hybrid Photo-Diode (HPD) tubes. To separate kaons from protons below 10 GeV/c an aerogel radiator will be used.

As an example of the usefulness of this device, Fig. 5.4 shows the efficiency for detecting the K^- in the decay $B_s \to D_s^+ K^-$ versus the rejection for the π^- in the decay $B_s \to D_s^+ \pi^-$. One sees that high efficiencies can be obtained with excellent rejections.

5.3.5 Electromagnetic Calorimeter

In BTeV, photons and electrons are detected when they create an electromagnetic shower in crystals of $PbWO_4$, a dense and transparent medium that produces scintillation light. The amount of light is proportional to the incident energy. The light is sensed by photomultiplier tubes (or possibly hybrid photodiodes). The crystals are 22 cm long and have a small transverse cross-section, 26 mm $\times$ 26 mm, providing excellent segmentation. The energy and position resolutions are exquisite,

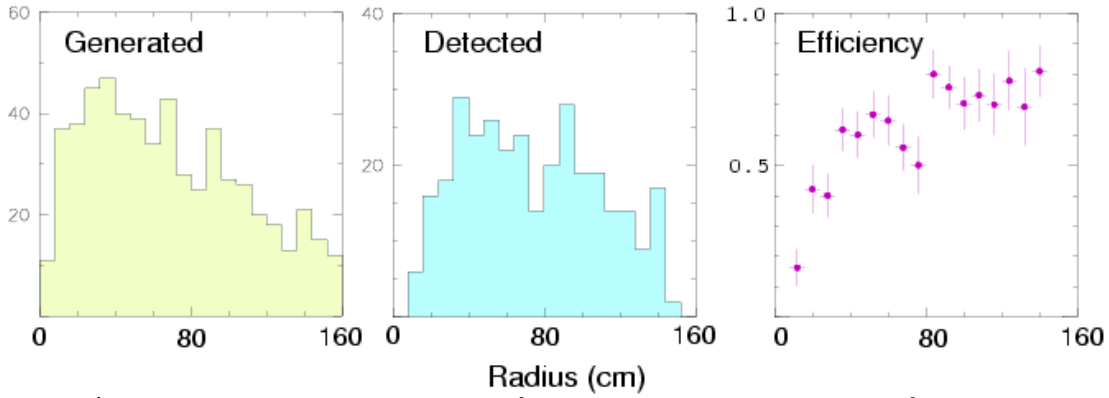

Figure 5.5: The radial distribution of generated and detected photons from $B^o \to K^*\gamma$ and the resulting efficiency. The detector response was simulated by GEANT and clusters of hit crystals were formed by the BTeV clustering software. This software is derived from software used for the Crystal Ball and CLEO experiments. The charged tracks from the K^* were required to hit the RICH. The simulation was run at 2 interactions/crossing.

$$\frac{\sigma_E}{E} = \sqrt{\frac{(1.6\%)^2}{E} + (0.55\%)^2}\ , \tag{5.1}$$

$$\sigma_x = \sqrt{\frac{(3500\ \mu m)^2}{E} + (200\ \mu m)^2}\ , \tag{5.2}$$

where E is in units of GeV. This leads to an r.m.s. π^o mass resolution between 2 and 5 MeV/c^2 over the π^o momentum range 1 to 40 GeV/c.

The crystals are designed to point at the center of the interaction region. They start at a radial distance of 10 cm with respect to the beam-line and extend out to 160 cm. They cover ~210 mrad. This is smaller than the 300 mrad acceptance of the tracking detector; the choice was made to reduce costs. For most final states of interest, this leads to a loss of approximately 20% in signal.

At 2 interactions per crossing the calorimeter has a high rate close to the beam pipe, where the reconstruction efficiency and resolution is degraded by overlaps with other tracks and photons. As one goes out to larger radius, the acceptance becomes quite good. This can be seen by examining the efficiency to reconstruct the γ in the decay $B^o \to K^*\gamma$, $K^* \to K^-\pi^+$. For this study the decay products of the K^* are required to reach the RICH detector. Fig. 5.5 shows the radial distributions of the generated γ's, the reconstructed γ's and the γ efficiency. The shower reconstruction code, described in Chapter 12 of the proposal, was developed from that used for the CLEO CsI calorimeter; for reference, the efficiency of the CLEO barrel electromagnetic calorimeter is 89%.

5.3.6 Forward Tracking System

The other components of the charged-particle tracking system are straw-tube wire proportional chambers and, near the beam where occupancies are high, silicon microstrip detectors.

These devices are used primarily for track momentum measurement, K_s detection and the Level 2 trigger. These detectors measure the deflection of charged particles by the BTeV analyzing magnet and give BTeV excellent mass and momentum resolution for charged particle decay modes.

5.3.7 Muon Detection

Muon detection is accomplished by insisting that the candidate charged track penetrate several interaction lengths of magnetized iron and insuring that the momentum determined from the bend in the toroid matches that given by the main spectrometer tracking system. The muon system is also used to trigger on the dimuon decays of the J/ψ. This is important not only to gather more signal but as a cross check on the efficiency of the main trigger, the Detached Vertex Trigger.

5.3.8 Data Acquisition System

BTeV has a data acquisition system (DAQ) which is capable of recording a very large number of events. The full rate of B's whose decay products are in the detector is very high, over 1 kHz. The rate from direct charm is similar. Some other experiments are forced by the limitations of their data acquisition system to make very harsh decisions on which B events to accept. BTeV can record nearly all the potentially interesting B and charm candidates in its acceptance. Therefore it can address many topics that might be discarded by an experiment whose DAQ is more restrictive. Since nature has a way of surprising us, the openness of the BTeV trigger and the capability of the DAQ are genuine strengths which permit the opportunity to learn something new and unanticipated.

5.4 Simulation and Analysis Tools

The physics reach of BTeV has been established by an extensive and sophisticated program of simulations, which is described in detail in Part III of the BTeV proposal [2]. For this study $p\bar{p} \to b\bar{b}X$ events were generated using `PYTHIA` [3] and the b hadrons were decayed using `QQ`. These packages are discussed in chapter 2 of this report. To model the detector response to these events, two detector simulation packages have been used, BTeVGeant and MCFast. BTeVGeant is a GEANT [4] based simulation of the BTeV detector which contains a complete description of the BTeV geometry including the materials needed for cooling, support and readout. GEANT models all physical interactions of particles with material and allows us to see the effects of hard to calculate backgrounds. Most of the results presented in this report were obtained using BTeVGeant. Some of the results presented here, and all earlier BTeV results, were obtained using MCFast [5], a fast parameterized simulation environment which allows the user to quickly change the detector design without the need to do any coding. BTeVGeant writes an MCFast geometry file which describes the same detector in simplified fashion; in this way the number, size and resolution of detector elements is synchronized between the two simulation tools. MCFast models the most of the

processes that GEANT does, energy loss, multiple scattering, pair creation, bremstrahlung, and hadronic interactions, but in a simplified fashion; for example some of the detector components are described by simpler shapes, the model of multiple scattering is purely gaussian and the model of energy deposition in the calorimeter is parametric.

Chapter 13 of the proposal shows quantitative comparisons between MCFast and BTeVGeant. From these studies one sees that MCFast is a reliable tool for computing resolutions, efficiencies and the level of backgrounds which arise from real tracks; the slower, more complete, BTeVGeant is necessary when occupancies and event confusion are the critical issues.

In most circumstances the simulations are done at the hit level, not at the digitization level. That is, the simulation packages produce smeared measurements, not a stream of device addresses and digitized pulse heights thta simulate the raw, experimental data stream. Digitization level simulations have been done to address the issue of required bandwidth at various levels of the trigger and DAQ systems.

For some of the physics studies presented in this report very high statistics Monte Carlo runs were required to reliably estimate the background level. These studies were performed on a farm of 500 MHz dual Pentium III Linux machines; over a period of 3 months an average of about 30 machines (60 CPUs) per day were available. To give one example, over a period of about 1 month, 4.5 million generic $b\bar{b}$ events were produced to investigate backgrounds in the channel $B^0 \to \rho\pi$.

Brief descriptions of simulation and analysis software for some specific subsystems were given in section 5.3 of this report. References to the relevant TDR sections were also given. In order to make this report a little more stand alone, a few more details are given below.

5.4.1 Tracking and Track Fitting Software

In both packages the simulation code keeps track of which tracking hits were created by which particles. This information is not used by the trigger code, which does full pattern recognition, but it is used to check the results of the trigger package and to debug it. Both simulation packages smear pixel hits using resolution functions with non-gaussian tails that were measured in the test beam. Hits in the other tracking detectors are modeled with gaussian resolution functions.

In the offline analysis package no pattern recognition is done; instead the Monte Carlo truth table is used to collect all of the hits which belong on a track. Each hit list is then Kalman filtered to give the track parameters and their covariance matrix in the neighborhood of the interaction region. Extrapolating from the excellent performance of the pattern recognition in the trigger, the final pattern recognition codes are expected to be be highly efficient and to find few false tracks; therefore the approximation of perfect pattern recognition gives a reliable estimate of what BTeV will achieve.

5.4.2 Electromagnetic Calorimeter Software

BTeVGeant does a complete development of electromagnetic and hadronic showers in all materials and follows the products of these showers into neighbouring detector volumes. When a track or photon within a shower traverses one of the $PbWO_4$ crystals, BTeVGeant deposits energy from that track or photon in the crystal. The total energy deposited in crystal is summed over each beam crossing and a parametric function is then used to convert the total deposited energy into a measured energy plus the error on the measured energy. For each crystal, a record is kept of how much energy was deposited for which track. This information is only used to characterize and debug the reconstruction code — it is not used by the reconstruction code.

When modelling shower development, it is necessary to stop tracing new particles when their energy drops below some cut-off. If these cut-off values are set too high, then the showers are too narrow, resulting in artificially clean events and artificially good energy resolution. If, on the other hand, these cut-off values are set too low, then simulations are prohibitively slow. The studies done to resolve of these tradeoffs are discussed in detail in Section 12.1.5 of the BTeV proposal. The final result is that, because adequate CPU power was available, no significant compromises in the quality of the simulation were necessary.

MCFast does the same calorimeter bookkeeping as BTeVGeant but the model of shower development is parametric, rather than a detailed following of each generation of particles. Both packages create identical data structures so that the same shower reconstruction and user analysis codes will work on events from both simulation packages.

5.4.3 Trigger Simulation Software

Chapter 9 of the proposal describes the overall plan for the trigger and it describes in detail the algorithm for the Level 1 Detached Vertex Trigger. This algorithm has been coded in C and is callable from by user code within either BTeVGeant or MCFast. A few pieces of the code have been ported to the target DSP's and carefully timed. The rest is written in a high level language for ease of algorithm development.

Similarly a prototype for the Level 2 trigger has also been coded. Since Level 2 will run on standard processes, the code represents a true prototype, and is not just a clone of the algorithm.

The physics analyses presented in the BTeV Proposal [2] and in this report have been used as models for possible Level 3 algorithms.

The trigger results presented in Table 5.1, and the results presented in chapters 6 through 8 were obtained using this trigger simulation software.

5.4.4 RICH Software

For most of the results presented in this workshop, nominal RICH efficiencies and misidentification probabilities were used. It was assumed that if a reconstructed track contained a

hit in the chambers between the RICH and the EMCal, then that track could be identified by the RICH.

In a few selected analyses, notably, $B_s \to D_s K$, a more detailed simulation was used. For this analysis tracks passing through the RICH generated photons which were propagated through the aerogel and chamber gas and reflected from the mirror. They were then propagated to the detector plan where a model of the HPD efficiency was applied. A pattern recognition algorithm was then run to find Cherenkov rings from the list of HPD hits. Particle ID decisions were made using these reconstructed rings. The physics reach predicted by these simulations is presented in chapter 6.

5.5 Flavor Tagging

Section 2.6 of this report describes the flavor tagging strategies which are available to B physics experiments at the Tevatron. In Chapter 15 of the BTeV proposal presents a preliminary study of the tagging power which can be achieved with the BTeV detector. This section will summarize the results of that study. Mixing of the opposite side B meson has not yet been included in the results shown here. The upcoming sections describe the algorithms used for tagging, and tagging powers which they achieve are summarized in Table 5.2.

5.5.1 Away Side Tagging

Three different away side tagging methods have been studied, lepton tagging, kaon tagging and vertex charge tagging. The first step in all three methods is to select tracks which are detached from all primary vertices in the event. In events with multiple primary vertices, detached tracks are only considered if they are associated with the same primary vertex as is the signal candidate.

5.5.1.1 Lepton Tagging

The lepton tagging algorithm must deal with possible wrong-sign tags which result from the cascade $b \to c \to \ell^+$. Because leptons from $b \to \ell^-$ and $b \to c \to \ell^+$ have quite different transverse momentum (p_T) distributions, good separation can be achieved. If there was more than one lepton tag candidate in an event, the highest p_T lepton was chosen to be the tag.

Candidates for muon tags were selected from the detached track list if they had a momentum greater than 4.0 GeV/c. A tagging muon with $p_T > 1.0$ GeV/c was considered to be from the process $b \to \ell^-$, while one with $p_T < 0.5$ GeV/c was considered to be from the process $b \to c \to \ell^+$, thereby flipping the sign of the tag.

Candidates for electron tags were selected using a parametrized electron efficiency and hadron misidentification probability. The tagging lepton was required to have $p_T > 1.0$

GeV/c and was always assumed to come from the process $b \to \ell^-$. There were not enough MC events to study electrons from $b \to c \to \ell^+$.

5.5.1.2 Kaon Tagging

Because of the large branching ratio for $b \to c \to K^- X$, kaon tagging is the most potent tagging method at e^+e^- B factories. At BTeV, in which the multiplicity of the underlying event is much greater, excellence in both particle identification and vertex resolution is required to exploit kaon tagging. Both are strong points of the forward detector geometry.

Candidates for kaon tags were selected from the secondary track list if they were identified as kaons in the RICH detector. If there was more than one kaon tag candidate in an event, the kaon with the largest normalized impact parameter with respect to the primary vertex was selected.

5.5.1.3 Vertex Charge Tagging

In this method a search was made for a detached vertex which is consistent with being from the charged decay products of the other b. The charge of that vertex determines the charge of the b. When the opposite side b hadronizes into a $\bar{B}^0$ or a $\bar{B}^0_s$, the tagging vertex has a neutral charge and there is no useful vertex tagging information in the event. However this method has the advantage that it is not affected by mixing of the away side b.

Tracks from the secondary list were accepted provided they had $p_T > 100$ MeV/c and provided they had $\Delta\eta < 4$ with respect to the direction of the signal B^0 candidate. The tracks from the secondary list were sorted into candidate vertices and only vertices with a detachment of at least $1.0\,\sigma$ from the primary vertex were accepted. If more than one vertex was found in an event, the one with the highest transverse momentum was selected; if no secondary vertices passed the selection cuts and if there was at least one track with $p_T > 1.0$ GeV/c, then the highest p_T track was selected. If the charge of the selected vertex is non-zero, then it determines the flavor of the away side b.

This tagging method is similar to jet charge tagging used by other experiments but BTeV has not yet investigated the possibility of weighting the tracks by their momenta.

5.5.1.4 Combining Away Side Tagging Methods

In many events, several of the same side tagging methods may give results; moreover it can happen that two methods will give contradictory answers. BTeV has not yet optimized the method of combining all tagging information but have used the following simple algorithm. The methods were polled in decreasing order of dilution and the first method to give an answer was accepted. That is, if lepton tagging gave a result, the result was accepted; if not, and if kaon tagging gave a result, the kaon tag was accepted; if not, and if the vertex charge tagging gave a result, the vertex charge tag was accepted.

5.5.2 Same Side Tagging

BTeV has studied the power of same side kaon tagging for B_s mesons. For this study tracks were selected provided they had a momentum greater than 3.0 GeV/c, were identified as kaons in the RICH and had an impact parameter with respect to the primary vertex less than 2 σ. It was further required that the system comprising the B_s candidate plus the candidate tagging track have an invariant mass less than 7.0 GeV/c^2. If more than one track passed these cuts, then the track closest in ϕ to the B_s direction was selected.

For same side tagging of B_d events BTeV expects to use B^{**} decays. This study is at an early, conceptual stage. The flag in Pythia to turn on B^{**} production has not been used. Instead BTeV has used a sample of simulated $B \to \psi K_s$ decays and has selected events in which the B and the next pion in the generator track list have an invariant mass in the range 5.6 - 5.8 GeV/c^2. It was assumed that 30% of these events will come from B^{**} decays and therefore be right sign tags. The remainder 70% of the events were assumed to have an equal number of right sign and wrong sign tags.

5.5.3 Summary of Tagging

The results from the tagging study are summarized in Table 5.2. These results are preliminary and one should be aware that all algorithms have yet to exploit the full power available to them. In particular, the vertexing information has yet to be fully exploited. For example, the $b \to \ell^-$ and $b \to c \to \ell^+$ samples differ not only in their p_T spectra; they have distinctly different topological properties. Similarly, kaon tagging can be improved if there is evidence that the kaon comes from a tertiary vertex, indicative of the $b \to c \to K^-$ cascade. Finally, the vertex charge algorithm should expect to find two vertices on the away side, the b decay vertex and the c decay vertex; the charge of both vertices provides tagging power. Other tagging methods have yet to be studied such as using a D^* from the decay of the opposite side B. Finally, we have not yet explored the optimal use of the correlations among all of the methods. Therefore, the results quoted in Table 5.2 probably underestimate the tagging power of BTeV, even though they do not yet incorporate mixing on the away side. Therefore the BTeV results quoted in this report are presented using nominal values of $\epsilon = 0.7$ and $D = 0.37$, giving $\epsilon D^2 = 0.1$. The studies presented in the present chapter should be regarded as evidence that these nominal values lie well within the ultimate reach of the experiment.

5.6 Schedule

The BTeV program is an ambitious one. Its goal is to begin data taking in 2005/6. This timing is well-matched to the world B physics program. The e^+e^- B factories and the Fermilab collider experiments will have had several years of running, the first results in, and their significance thoroughly digested. It should be clear what the next set of goals is and BTeV will be guaranteed to be well-positioned to attack them. This schedule also gives BTeV a good opportunity to have a head start in its inevitable competition with LHC-b,

Tag Type	ϵ	D	ϵD^2
Muon	4.5%	0.66	2.0%
Electron	2.3%	0.68	1.0%
Kaon	18%	0.52	4.9%
Vertex Charge	32%	0.36	4.1%
Same Side Kaon	40%	0.26	2.6%
Same Side Pion	88%	0.16	2.2%
Total for B_s			14.6 %
Total for B_d			14.2 %
Total for B_s with overlaps	65%	0.37	8.9%

Table 5.2: Results of first generation studies of tagging power in BTeV. In the text it is discussed that these studies are incomplete and that they likely underestimate the tagging power which can be realized.

especially since BTeV can be installing and operating components of its detector in the collision hall well in advance of 2005. Finally, this schedule is sensibly related to BTeV's plan to conduct a rigorous R&D program which includes a sequence of engineering runs to test the technically challenging systems in the BTeV design. We believe that the scale of the BTeV construction effort is comparable to the scale of one of the current detector upgrades. The time scale is comparable as well.

5.7 Conclusions

BTeV is a powerful and precise scientific instrument capable of exquisite tests of the Standard Model. It has great potential to discover new physics via rare or CP violating decays of heavy quarks. Details of the physics reach of BTeV and can be found in chapters 6 through 9 of this report and a summary table can be found in the executive summary [6] of the BTeV Proposal.

References

[1] A list of the BTeV Collaboration can be found in Ref. [2].

[2] "Proposal for an Experiment to Measure Mixing, CP Violation and Rare Decays in Charm and Beauty Particle Decays at the Fermilab Collider — BTeV", Fermilab, May 2000. This is available at the URL, `http://www-btev.fnal.gov/public\_documents/btev\_proposal`.

[3] H. U. Bengtsson and T. Sjostrand, Comp. Phys. Comm. **46**, 43 (1987).

[4] GEANT: CERN Program Library Long Writeup W5013, `http://wwwinfo.cern.ch/asdoc/geant\_html3/geantall.html`.

[5] P. Avery *et al.*, "MCFast: A Fast Simulation Package for Detector Design Studies", in the Proceedings of the International Conference on Computing in High Energy Physics, Berlin, (1997). Documentation can be found at `http://www-cpd.fnal.gov/mcfast.html`.

[6] The executive summary is part of the BTeV Proposal, Ref. [2] and can be found separately on the BTeV Proposal web page.